Angiogenesis (2016) 19:245–254
DOI 10.1007/s10456-016-9499-4

BRIEF COMMUNICATION

In situ validation of VEGFR-2 and $\alpha_v\beta_3$ integrin as targets for breast lesion characterization

Josef Ehling[1,2] · Matthias Misiewicz[1] · Saskia von Stillfried[2] · Diana Möckel[1] · Jessica Bzyl[1] · Sibylle Pochon[3] · Wiltrud Lederle[1] · Ruth Knuechel[2] · Twan Lammers[1,4,5] · Moritz Palmowski[1] · Fabian Kiessling[1]

Received: 19 August 2015 / Accepted: 11 February 2016 / Published online: 22 February 2016

Abstract Vascular endothelial growth factor receptor 2 (VEGFR-2) and $\alpha_v\beta_3$ integrin are the most frequently addressed targets in molecular imaging of tumor angiogenesis. In preclinical studies, molecular imaging of angiogenesis has shown potential to detect and differentiate benign and malignant lesions of the breast. Thus, in this retrospective clinical study employing patient tissues, the diagnostic value of VEGFR-2, $\alpha_v\beta_3$ integrin and vascular area fraction for the diagnosis and differentiation of breast neoplasia was evaluated. To this end, tissue sections of breast cancer ($n = 40$), pre-invasive ductal carcinoma in situ (DCIS; $n = 8$), fibroadenoma ($n = 40$), radial scar ($n = 6$) and normal breast tissue ($n = 40$) were used to quantify (1) endothelial VEGFR-2, (2) endothelial $\alpha_v\beta_3$ integrin and (3) total $\alpha_v\beta_3$ integrin expression, as well as (4) the vascular area fraction. Sensitivity and specificity to differentiate benign from malignant lesions were calculated for each marker by receiver operating characteristics (ROC) analyses. Whereas vessel density, as commonly used, did not significantly differ between benign and malignant lesions (AUROC: 0.54), VEGFR-2 and $\alpha_v\beta_3$ integrin levels were gradually up-regulated in carcinoma versus fibroadenoma versus healthy tissue. The highest diagnostic accuracy for differentiating carcinoma from fibroadenoma was found for total $\alpha_v\beta_3$ integrin expression (AUROC: 0.76), followed by VEGFR-2 (AUROC: 0.71) and endothelial $\alpha_v\beta_3$ integrin expression (AUROC: 0.68). In conclusion, total $\alpha_v\beta_3$ integrin expression is the best discriminator between breast cancer, fibroadenoma and normal breast tissue. With respect to vascular targeting and molecular imaging of angiogenesis, endothelial VEGFR-2 appeared to be slightly superior to endothelial $\alpha_v\beta_3$ for differentiating benign from cancerous lesions.

Keywords Molecular imaging · Breast cancer screening · Mammography · BR55 · RGD

Introduction

Breast cancer is the second leading cause of cancer-related deaths among women in the USA and Europe [1, 2]. Although annual X-ray mammography screening was reported to result in a reduction of breast cancer-related mortality [3], radiation exposure is high and/or the diagnostic accuracy can be impaired by high tissue density or by nonmalignant sclerotic lesions such as radial scars associated with a carcinoma-mimicking spiculated appearance. Therefore, mammography is usually supplemented by an ultrasound examination providing a different tissue contrast. Whereas surgical resection is standard

Electronic supplementary material The online version of this article (doi:10.1007/s10456-016-9499-4) contains supplementary material, which is available to authorized users.

✉ Fabian Kiessling
fkiessling@ukaachen.de

[1] Department for Experimental Molecular Imaging, Helmholtz Institute for Biomedical Engineering, Medical Faculty, RWTH Aachen University, Pauwelsstr. 30, 52074 Aachen, Germany

[2] Institute of Pathology, Medical Faculty, RWTH Aachen University, Aachen, Germany

[3] Bracco Suisse SA, Geneva, Switzerland

[4] Department of Targeted Therapeutics, MIRA Institute for Biomedical Technology and Technical Medicine, University of Twente, Enschede, The Netherlands

[5] Department of Pharmaceutics, Utrecht Institute for Pharmaceutical Sciences, Utrecht University, Utrecht, The Netherlands

treatment in case of evident cancer-suspect findings or high-grade ductal carcinoma in situ (DCIS), follow-up controls are recommended in case of diagnostic findings associated with benign lesions (e.g., fibroadenoma) or sclerotic lesions such as radial scars. Intricately, in case of uncertain or conflicting mammography/sonography findings, the execution of an (ultrasound-guided) biopsy is routinely performed for the diagnostic clarification of the suspect finding [4]. However, biopsies are painful and carry the risk of tumor cell retraction in the biopsy channel. Thus, it would be highly helpful to get higher diagnostic accuracy for uncertain lesions by the ultrasound examination, which would reduce the number of required biopsies and avoid the application of another cost- and time-intensive imaging method such as dynamic contrast-enhanced magnetic resonance imaging (DCE-MRI).

The use of molecularly targeted microbubbles as contrast agents may move ultrasound imaging toward the required sensitivity and specificity. In this regard, angiogenesis-associated proteins expressed on the endothelial cell layer such as VEGFR-2 and $\alpha_v\beta_3$ integrin have been identified as promising targets for monitoring (anti-)angiogenesis using molecularly targeted microbubbles in combination with ultrasound imaging in preclinical tumor models [5, 6]. Whereas the transmembrane receptor tyrosine kinase VEGFR-2, which activates the PI3K/Akt/mTOR pathway and mediates endothelial cell proliferation, is mainly expressed on activated endothelium, the cell adhesion molecule $\alpha_v\beta_3$ integrin, which binds to arginine-glycine-aspartic acid (RGD)-containing proteins and peptides, is upregulated on tumor endothelium and on interstitial and tumor cells [7–9]. Importantly, as reported by previous studies [10–12], molecular ultrasound enables the noninvasive discrimination between breast neoplasms of different malignancy in mice and rats. In addition, phase II clinical trials have been recently launched evaluating the diagnostic potential of VEGFR-2-targeted microbubbles (BR55) using ultrasound in patients with breast or ovarian cancer (www.clinicaltrialsregister.eu, EudraCT: 2012-000699-40) and prostate cancer (www.clinicaltrials.gov, NCT02142608). However, results from translational trials investigating the diagnostic accuracy of molecular ultrasound contrast agents targeting VEGFR-2 for breast tumor differentiation have not yet been published.

$\alpha_v\beta_3$ integrin has also been reported previously to be expressed on the endothelium in malignant tumors, thus rendering it promising as a target molecule for molecular ultrasound imaging purposes using $\alpha_v\beta_3$-targeting microbubbles [13]. However, the majority of preclinical molecular imaging studies focusing on targeted $\alpha_v\beta_3$ integrin imaging utilize RGD-based peptides for positron emission tomography (PET) or single-photon emission computed tomography (SPECT) imaging [14–16]. Results from translational trials investigating the diagnostic accuracy of (1) molecular ultrasound contrast agents targeting endothelial $\alpha_v\beta_3$ integrin or (2) molecular PET or SPECT contrast agents targeting globally expressed $\alpha_v\beta_3$ integrin for breast tumor differentiation have only rarely been reported so far [17–19].

Here, we evaluated the suitability of the molecular imaging targets VEGFR-2 and $\alpha_v\beta_3$ integrin for the clinical discrimination between benign and malignant lesions using tissue samples of 134 female patients with ductal cancer, lobular cancer, high-grade DCIS, benign fibroadenoma, radial scars and healthy breast tissue (Table 1). Furthermore, we compared the sensitivity and specificity of VEGFR-2 and $\alpha_v\beta_3$ integrin expression with those of the vascular area fraction (upon computational filling of CD31-positive vessel structures), in order to investigate the diagnostic precision of these targets for differentiating suspicious breast lesions, e.g., with molecular imaging methods.

Materials and methods

Human tissue samples

Tissue samples from 134 female patients were evaluated to quantify the VEGFR-2 and $\alpha_v\beta_3$ integrin expression as well as the vascular area fraction in breast cancer, DCIS, benign fibroadenoma, radial scar and normal breast tissue

Table 1 Patient characteristics

	No. of patients
Normal breast	40
Fibroadenoma	40
Radial scar	6
Ductal carcinoma in situ (DCIS)	8
Breast carcinoma	40
Histologic type	
Ductal cancer	20
Lobular cancer	20
Histologic grade	
G1	2
G2	25
G3	13
Tumor size	
$T \leq 2$ cm	24
$T > 2$ cm	16
Lymph node involvement	
Positive	5
Negative	34
Missing	1

specimens. In accordance with their histomorphological subtype (Table 1), $n = 40$ breast cancer patients (64 ± 12 years) were subdivided into patients with ductal cancer ($n = 20$; 67 ± 12 years) and lobular cancer ($n = 20$; 60 ± 10 years). Patients undergoing neo-adjuvant therapy were not included. Representing a precancerous but noninvasive lesion, $n = 8$ patients with high-grade DCIS were selected (56 ± 12 years). Representing benign lesions, $n = 40$ patients with fibroadenoma (30 ± 10 years) and $n = 6$ patients with radial scars (52 ± 13 years) were selected. All investigated tissues were taken from vital areas in the periphery of the lesions. Normal breast tissue samples were obtained from breast reduction surgery specimens ($n = 40$; 42 ± 17 years). The use of human tissue was approved by the local ethics committee of the RWTH Aachen University. The diagnostic appraisal was performed by experienced pathologists and based on clinical pathological guidelines.

Quantitative immunofluorescence and statistical analyses

Immunofluorescent stainings for CD31, VEGFR-2 and $\alpha_v\beta_3$ integrin were performed using routine protocols. Prior to immunofluorescence staining, paraffin-embedded tissue samples were pre-treated with ultraviolet light for 3 h (at 515 and 630 nm) to reduce collagen auto-fluorescence without affecting tissue integrity. Subsequently, paraffin-embedded tissue sections were processed using routine protocols and co-stained for CD31 (Acris antibodies, Herford, Germany) and VEGFR-2 (Dianova, Hamburg, Germany) or for CD31 and $\alpha_v\beta_3$ integrin (Abcam, Cambridge, United Kingdom). Cy2- and Cy3-labeled secondary antibodies were obtained from Dianova. Counterstaining of cell nuclei was performed using Hoechst 33258 (Sigma-Aldrich, Steinheim, Germany).

Fluorescence microscopy was performed using an Axio Imager M2 microscope with an AxioCam MRm revision 3 high-resolution camera (Carl Zeiss, Göttingen, Germany). Four different fields-of-view (FOVs; each 225 × 170 μm^2) per section were captured representatively. Comparable exposure times per channel were used for all tissue sections. Fluorescence signals of endothelial VEGFR-2 as well as of total and endothelial $\alpha_v\beta_3$ integrin expressions were segmented based on threshold, and area fractions were analyzed using the AxioVision Rel 4.8 software (Carl Zeiss). Comparable thresholds per channel were used for all tissue sections. When specifically quantifying the endothelial area fraction of VEGFR-2 or $\alpha_v\beta_3$ integrin, all threshold-based segmented but nonendothelial (CD31) co-localized signals were manually excluded (Supplementary Fig. S1a+b). The vascular area fraction was computationally reconstructed by filling all CD31-positive vascular structures using a previously described custom macro implemented for open-access ImageJ analysis software version 1.43ru (NIH; Bethesda, MD, USA) (Supplementary Fig. S1c) [20].

Statistical analysis

Data are shown as scattered dot plots including median with interquartile range. The nonparametric Kruskal–Wallis test combined with Dunn's multiple comparison test was used to compare (1) the filled CD31 area fraction, (2) the endothelial VEGFR-2 expression, (3) the total $\alpha_v\beta_3$ expression and (4) the endothelial $\alpha_v\beta_3$ expression across various patient groups or various grades of carcinomas. For comparing these parameters between IDC and ILC or between different tumor sizes, the nonparametric Mann–Whitney test was used. A P value of <0.05 was considered significant. Sensitivity and specificity were assessed using receiver operating characteristics (ROC) analyses. Area under the ROC curve (AUROC) was calculated to compare the diagnostic accuracy of the above-mentioned parameters for differentiating histologic breast entities. Statistical analyses were performed using GraphPad Prism 5.0 (GraphPad Software, San Diego, CA, USA).

Results

Endothelial VEGFR-2 levels, but not vascular area fractions, enable the discrimination between malignant and benign breast lesions

We first analyzed the endothelial VEGFR-2 expression in specimens of normal breast tissue versus fibroadenoma versus carcinoma, and compared VEGFR-2 levels with vascular area fractions as a marker of vascularization (Fig. 1a and Supplementary Fig. 2a). Quantifications of the filled CD31 area fraction as a histologically reconstructed measure for the vascular area fraction merely revealed significant differences between normal breast tissue and any sort of neoplasm ($P < 0.001$; Fig. 1b). Values for the filled CD31 area fraction did not significantly differ between fibroadenoma (7.6 ± 1.9 %; Fig. 1b), DCIS (7.0 ± 1.3 %; Supplementary Fig. 2b) and carcinoma (7.9 ± 2.4 %; Fig. 1b). These findings indicate that the discrimination between cancerous, pre-invasive DCIS and benign lesions could not be achieved by quantifying the vascular area fraction, which seems to be generally increased in any sort of breast neoplasms. Merely, the filled CD31 area fraction was significantly lower in radial scars than in fibroadenoma or carcinoma ($P < 0.01$; cf. Fig. 1b and Supplementary Fig. 2b).

Conversely, endothelial VEGFR-2 expression increased in breast cancer by +171 % compared to normal breast

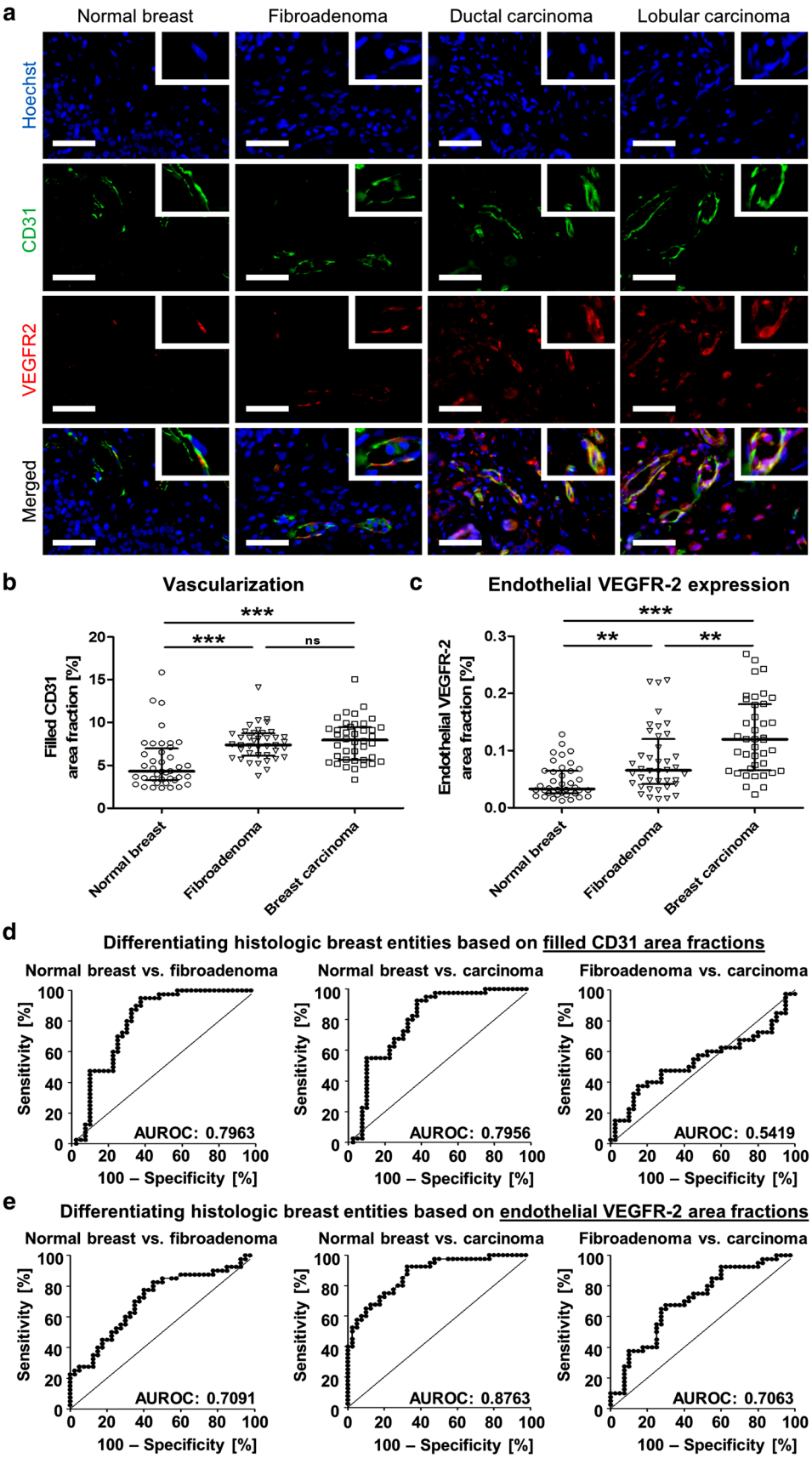

Fig. 1 Vascular area fraction and endothelial VEGFR-2 expression in different neoplastic lesions of the human breast. **a** Representative photomicrographs of normal breast tissue (*first column*), fibroadenoma (*second column*), ductal carcinoma (*third column*) and lobular carcinoma (*fourth column*) co-stained with Hoechst cell nuclei marker (*blue*, *first row*), against endothelial cell marker CD31 (*green*, *second row*) and against VEGFR-2 (*red*, *third row*). Merged images (*fourth column*) demonstrate that VEGFR-2 was expressed by CD31-positive endothelial cells and, in parts, aberrantly by tumor cells. *Scale bar* = 50 µm. Quantification of the filled CD31 (**b**) and endothelial VEGFR-2 (**c**) area fraction in all cohorts. Data are shown as *scattered dot plots* including median with interquartile range; $n = 40$ patients per group; *** $P < 0.001$ and ** $P < 0.01$ (Kruskal–Wallis test including Dunn's multiple comparison test). **d**+**e** ROC curves for differentiating invasive breast cancer from benign entities (normal breast and fibroadenoma). ROC analyses were performed based on quantified area fractions of the computationally filled CD31 signal reflecting the vascular area fraction (**d**) and of the endothelial VEGFR-2 signal (**e**) using immunofluorescence for differentiating normal breast versus fibroadenoma (*left panels*), normal breast vs. carcinoma (*middle panels*) and fibroadenoma versus carcinoma (*right panels*; $n = 40$ patients per group). Note that the diagnostic accuracy, reflected by the calculated area under ROC curve (AUROC), is significantly higher for a VEGFR-2-based discrimination between cancerous lesions and fibroadenomatous hyperplasia than for vascular area fraction-based discrimination

tissue (0.125 ± 0.065 % vs. 0.046 ± 0.056 % VEGFR-2 area fraction, respectively; $P < 0.0001$; Fig. 1c), by +138 % compared to radial scars (0.0525 ± 0.01643 %; Supplementary Fig. 2c) and by +52 % compared to fibroadenoma (0.082 ± 0.056 %; $P < 0.01$; Fig. 1c). This demonstrates that endothelial VEGFR-2 is gradually up-regulated in breast neoplasms, i.e., a slight up-regulation in benign fibroadenoma and a stronger up-regulation in malignant carcinomas, confirming the usefulness of endothelially expressed VEGFR-2 as a diagnostic target for discriminating malignant and benign breast lesions (e.g., using VEGFR-2-targeted molecular imaging agents, such as BR55). Importantly, compared to normal breast tissue, significant higher values for the endothelial VEGFR-2 area fraction were also found in situ for DCIS lesions (0.1066 ± 0.01899 %; $P < 0.01$; cf. Figure 1c and Supplementary Fig. 2c). Interestingly, no significant differences were observed when comparing breast cancer subtypes, such as ductal cancer and lobular cancer, neither for the filled CD31 nor for the endothelial VEGFR-2 area fraction (Supplementary Fig. S3a+b). Moreover, with the exception of filled CD31 area fraction in carcinoma grouped by tumor size, neither vascular area fraction nor VEGFR-2 expression did significantly differ when comparing different tumor grades and sizes with each other (Supplementary Fig. S4+5).

To test our hypothesis that endothelial VEGFR-2 better discriminates between benign and malignant breast lesions than vessel density, ROC analyses were carried out by representatively taking results from normal breast tissue, benign fibroadenoma and breast carcinoma into account. Overall, quantifying the filled CD31 area fraction merely allowed the differentiation between normal breast tissue and any sort of neoplasm with high diagnostic accuracy (AUROC: 0.79), but not a valid discrimination between benign and malignant lesions (AUROC: 0.54; Fig. 1d; Supplementary Table S1+2). Strikingly, quantifying the endothelial VEGFR-2 expression allowed in particular this clinically relevant discrimination between noncancerous and cancerous breast lesions with significantly increased diagnostic accuracy (AUROC: 0.71; Fig. 1e; Supplementary Table S3+4). At an optimal discrimination cutoff of 0.09 % endothelial VEGFR-2 area fraction, benign and malignant breast lesions were predicted to be diagnosed with a sensitivity of 67.5 % and a specificity of 70 % (as compared to merely 55 % for both sensitivity and specificity at a cutoff of 7.710 % for the filled CD31 area fraction) (cf. Supplementary Table S1 with S3). In addition, as expected, only a weak but significant correlation was found in carcinoma patients when comparing the area fractions of filled CD31-positive vessels with those of endothelial VEGFR-2 expression (the Pearson $r = 0.3297$; $P < 0.05$; Supplementary Fig. S6). Collectively, these findings indicate that VEGFR-2, expressed on the activated endothelium, may be indicated as a molecular imaging target for the discrimination between cancerous or pre-invasive versus noncancerous breast lesions and superior to the assessment of vascularization.

Endothelial and total $\alpha_v\beta_3$ integrin expression

To further investigate if $\alpha_v\beta_3$ integrin, another preclinically validated target molecule for molecular imaging, is also suitable for the clinical discrimination between cancerous, pre-invasive DCIS and benign breast lesions, tissue samples of 134 patients were stained against CD31 and $\alpha_v\beta_3$ integrin (Fig. 2a and Supplementary Fig. S2d). Representative images demonstrate that in line with VEGFR-2, which is predominantly but not exclusively expressed by endothelial cells (Fig. 1a) [21, 22], $\alpha_v\beta_3$ integrin is expressed by endothelial, stromal and breast cancer cells (Fig. 2a). Significant differences in the total $\alpha_v\beta_3$ integrin area fraction (combining endothelial and nonendothelial $\alpha_v\beta_3$ integrin and thus being more relevant for extravasating molecular imaging probes) were observed between benign fibroadenoma (3.7 ± 1.3 % total $\alpha_v\beta_3$ area fraction) and normal tissue (2.7 ± 0.6 %; $P < 0.001$; Fig. 2b). Importantly, differences in total $\alpha_v\beta_3$ area fraction were also significant when comparing invasive breast cancer (4.8 ± 1.1 %) with benign breast lesions such as fibroadenoma (3.7 ± 1.3 %; $P < 0.001$; Fig. 2b) or radial scars (2.4 % ± 0.4 %; $P < 0.001$; Supplementary Fig. S2e). Moreover, a significant difference was also observed for the total $\alpha_v\beta_3$ area fraction when comparing pre-invasive DCIS lesions (3.2 ± 0.7 %) with invasive cancerous breast lesions (Supplementary Fig. S2e; $P < 0.05$).

Importantly, entity-specific differences were smaller for endothelial expression of $\alpha_v\beta_3$ integrin, which is only relevant for large-sized intravascularly circulating microbubbles, when comparing normal tissue with fibroadenoma or carcinoma (0.04 ± 0.01 % vs. 0.06 ± 0.02 % vs. 0.08 ± 0.03 % endothelial $\alpha_v\beta_3$ area fraction; $P < 0.05$) (Fig. 2c). An up-regulation of the endothelial $\alpha_v\beta_3$ integrin expression was neither found in radial scars nor in pre-invasive DCIS lesions (Supplementary Fig. S2f).

When evaluating the endothelial and total $\alpha_v\beta_3$ integrin expression for differentiating between benign and cancerous lesions using ROC analyses, it was found that, as compared to VEGFR-2, the diagnostic accuracy of endothelial $\alpha_v\beta_3$ integrin was lower (AUROC: 0.68; Supplementary Fig. S7; Supplementary Table S5+6) and totally expressed $\alpha_v\beta_3$ integrin was higher (AUROC: 0.76; Fig. 2d; Supplementary Table S7+8). However, the diagnostic accuracies of both, endothelial and global $\alpha_v\beta_3$ integrin, were significantly higher compared to the diagnostic accuracy of the vascular area fraction (AUROC:

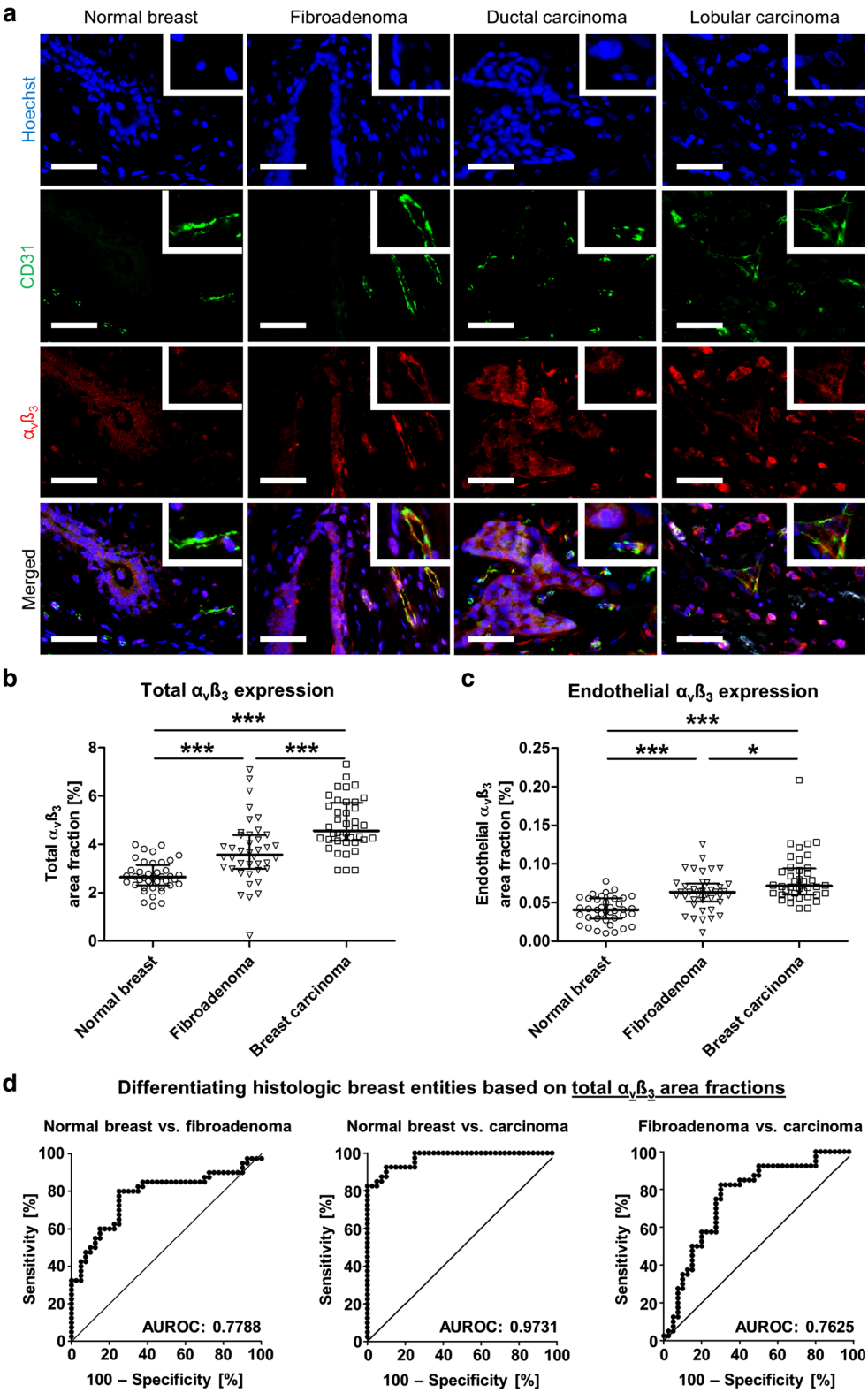

Fig. 2 Total and endothelial $\alpha_v\beta_3$ integrin expressions in different neoplastic lesions of the human breast. **a** Representative immunofluorescence microscopy images of normal breast tissue (*first column*), fibroadenoma (*second column*), ductal carcinoma (*third column*) and lobular carcinoma (*fourth column*) co-stained with Hoechst cell nuclei marker (*blue*, *first row*), against endothelial cell marker CD31 (*green*, *second row*) and against $\alpha_v\beta_3$ integrin (*red*, *third row*). Merged images (*fourth column*) demonstrate that $\alpha_v\beta_3$ integrin is expressed by endothelial cells, but also by mesenchymal and epithelial/tumor cells. *Scale bar* = 50 µm. Quantification of the total (**b**) and the endothelial $\alpha_v\beta_3$ integrin (**c**) area fraction in all cohorts. Data are shown as *scattered dot plots* including median with interquartile range; $n = 40$ patients per group; *** $P < 0.001$ and ** $P < 0.01$ (Kruskal–Wallis test including Dunn's multiple comparison test). (**d**) ROC analyses based on the total $\alpha_v\beta_3$ integrin signal for differentiating normal breast versus fibroadenoma (*left panels*), normal breast versus carcinoma (*middle panels*) and fibroadenoma versus carcinoma (*right panels*; $n = 40$ patients per group)

0.54; Fig. 1d). At an optimal cutoff of 0.065 % endothelial $\alpha_v\beta_3$ integrin area fraction, benign and malignant breast lesions were predicted to be diagnosed with a sensitivity of 67.5 % and a specificity of 62.5 % (Supplementary Table S5). Higher values for sensitivity (82.5 %) and specificity (70 %) were found for totally expressed $\alpha_v\beta_3$

integrin, at a threshold level of 4.06 % (Supplementary Table S7). Importantly, when comparing the diagnostic accuracies of the three markers for differentiating between cancer and normal breast tissue using ROC analyses, total $\alpha_v\beta_3$ integrin (AUROC: 0.97; Fig. 2d) and endothelial $\alpha_v\beta_3$ integrin (AUROC: 0.92; Supplementary Fig. S7) were both associated with a higher diagnostic accuracy than endothelial VEGFR-2 (AUROC: 0.87; Fig. 1e). Notably, neither the total nor endothelial area fraction of $\alpha_v\beta_3$ integrin significantly differed when comparing ductal cancer with lobular cancer (Supplementary Fig. S3c+d). In addition, levels of endothelial and global $\alpha_v\beta_3$ integrin did not significantly differ when comparing different tumor grades or sizes with each other (Supplementary Fig. S4+5).

Discussion

Clinically applicable molecular imaging technologies such as ultrasound, MRI, PET and SPECT, which allow noninvasive quantitative analyses of marker molecules on tumor, vascular and stromal cells, are considered promising for diagnosing and staging malignancies as well as for therapy monitoring. With respect to breast cancer, several studies have demonstrated the high diagnostic potential of molecular imaging approaches using VEGFR-2 or $\alpha_v\beta_3$-targeted contrast agents in preclinical tumor models [5, 6, 10–12, 23–25]. However, besides a pilot phase study on breast cancer patients using radiolabeled $\alpha_v\beta_3$-targeted RGD peptides and PET demonstrating a significant probe uptake in the primary lesion and in the metastases [19], clinical studies comparing the diagnostic power of functional versus molecular imaging for differentiating (mammographically) suspect tumors or for monitoring recurrent lesions upon breast cancer surgery have not yet been reported. Though a clinical study investigating the diagnostic accuracy of molecular ultrasound imaging using VEGFR-2-targeted microbubbles (BR55) for breast tumor discrimination has been performed (EudraCT: 2012-000699-40), the final conclusions are not yet disclosed.

To bridge this gap on the histopathological level, we aimed to systematically compare vascularization- and angiogenesis-based parameters regarding their diagnostic potential to discriminate between cancer, pre-invasive DCIS, nonmalignant breast lesions and normal breast tissue. We found that several breast lesions such as breast cancer, pre-invasive DCIS and fibroadenoma were all unspecifically associated with increased vascularization levels (reflected by increased vascular area fractions) compared to normal breast tissue, but no significant differences were observed between cancerous and benign lesions, indicating that a vascularization-derived parameter such as the vascular area fraction alone is not sufficient enough to distinguish between both entities. Partially contradicting results previously made by Wells et al. [26] and Bluff et al. [27], who found significant higher vascularization levels in breast carcinomas compared to benign fibroadenomas or DCIS lesions, might be explained by the fact that they quantified the microvessel density (MVD) [28] as a measure of tissue vascularization, whereas we reconstructed the vascular area fraction (via computationally filling all CD31-positive vessels) because this parameter reflects more closely functional vascularization parameters (e.g., the relative blood volume, rBV) as they are usually in vivo determined in patients. Although differences in the vascular area fraction were not significant yet between invasive cancer and benign breast lesions or pre-invasive DCIS lesions, a tendency toward increased vascularization levels in breast cancer was also observed in the patient cohorts analyzed in our study. These differences would potentially become significant when increasing the sample size. However, this would not provide much benefit for the vascular area fraction as a diagnostic parameter due to a very limited discriminatory power accompanied by a high number of false positive and/or negative results. In addition, one has to consider that within our study only a histological measure of the vascular volume was assessed. With respect to vessel functionality, better results obtained by DCE-MRI [29, 30] may be explained by the functional nature of the parameters (e.g., peak enhancement and washout), which, besides the blood volume, are also influenced by perfusion, vascular leakage and enhanced interstitial retention of the contrast agent. In contrast, we found that the expression of the pro-angiogenic marker proteins VEGFR-2 and $\alpha_v\beta_3$ integrin differed significantly between breast cancer, pre-invasive cancerous lesions and benign breast lesions. In line with preclinical studies, our histopathological in situ findings support the notion that VEGFR-2 and $\alpha_v\beta_3$ integrin may be suitable molecular imaging targets for tumor diagnosis and characterization in the breast [5, 6, 10–12, 23–25].

The addition of molecularly targeted imaging procedures to mammography for characterizing suspect breast lesions has been shown to improve specificity of the diagnostic evaluation and to reduce the number of unnecessary biopsies [31]. Based on preclinical reports, potential molecular imaging devices might be based on intravascularly circulating molecularly targeted microbubbles accessing molecular targets on the luminal surface of the activated endothelium in tumors, or might be based on small-sized extravasating peptides targeted against aberrantly expressed proteins on the surface of cancer cells or cancer-associated (stromal) cells. Whereas the former ones include, i.e., molecular ultrasound in combination with microbubbles targeted against endothelially expressed angiogenesis-related proteins such as VEGFR-2 or $\alpha_v\beta_3$ integrin, the latter ones include, i.e., PET and SPECT combined with RGD-based peptides [13–19].

With respect to ultrasound imaging, the use of molecularly targeted microbubbles as contrast agents may move the combinational application of ultrasound plus mammography for characterizing suspect breast lesions toward higher levels of sensitivity and specificity and would thus reduce the number of unnecessary biopsies. However, while whole-breast screening using ultrasound has been suffering from high operator-dependence for years [32], recent technological developments in automated 3D breast sonography (resulting in reduced interobserver variability) significantly promote the applicability of whole-breast ultrasound as a screening tool [31, 33]. In this context, molecular ultrasound imaging, which utilizes intravenously injected microbubbles targeted against angiogenesis marker proteins expressed on the luminal surface of activated endothelium, might become a fast operable and low-cost addition to the diagnostic evaluation of breast masses using sonography (in contrast to DCE-MRI, PET or SPECT). Referring to this, our in situ data indicate that endothelial VEGFR-2 may be superior to endothelial $\alpha_v\beta_3$ integrin for the differentiation of benign versus malignant breast tumors using targeted microbubbles and molecular ultrasound.

Due to the fact that $\alpha_v\beta_3$ integrin is not only expressed by activated endothelial cells but also by breast cancer cells and cancer-associated activated stromal cells, within our histopathological study, total $\alpha_v\beta_3$ integrin has been identified as the best discriminator between invasive breast cancer, pre-invasive DCIS, benign lesions (radial scars, fibroadenoma) and normal breast tissue. Consequently, compared to endothelial VEGFR-2 and endothelial $\alpha_v\beta_3$ integrin expression, total $\alpha_v\beta_3$ integrin was presented with the highest diagnostic accuracy for detecting and differentiating breast lesions, indicating that, in principle, total $\alpha_v\beta_3$ integrin may be superior to the former two markers. These data are in line with numerous previous studies reporting on (1) $\alpha_v\beta_3$ integrin as a prognostic indicator in breast cancer [34], (2) the pharmaceutical targeting of $\alpha_v\beta_3$ integrin to increase the efficacy of radioimmunotherapy in breast cancer [35], (3) the contribution of $\alpha_v\beta_3$ integrin to tumor progression and metastatic potential [36] as well as (4) its contribution as a driver of cancer stemness and drug resistance in the neoplastic mammary gland [37, 38]. However, $\alpha_v\beta_3$ integrin expressed on cancer and/or stromal cells cannot be actively targeted using intravascularly circulating microbubbles but merely by small-sized RGD-based probes. These, however, would require the combination with PET- or SPECT-based molecular imaging techniques, which are more time- and cost-intensive than ultrasound.

In conclusion, this study bridges the gap between research on molecular imaging in preclinical breast cancer models and clinical studies using angiogenesis-targeted contrast agents for noninvasively differentiating suspect breast lesions. Our histopathological findings demonstrate that a purely vascular area fraction-based discrimination between malignant and benign breast lesions may be insufficient due to highly variable vascularization levels found in both entities. Secondly, VEGFR-2 and $\alpha_v\beta_3$ integrin expression are significantly higher in human breast cancer and pre-invasive DCIS lesions than in benign lesions (e.g., fibroadenoma or radial scars) or normal breast tissue, making them both in principle suitable as targets for molecular imaging. With respect to vascular targeting, which is more relevant for targeted ultrasound imaging, endothelial VEGFR-2 might be more suitable than endothelial $\alpha_v\beta_3$ for differentiating benign from malignant breast tumors. On the contrary, with respect to small probes enabling the targeting of stromal and tumor cells, total $\alpha_v\beta_3$ integrin has been identified as the best discriminator between breast cancer, benign lesions and normal breast tissue. Thus, $\alpha_v\beta_3$ integrin might be highly suitable for breast tumor detection and therapy monitoring using RGD-based probes, e.g., for PET and SPECT.

Acknowledgments This work was supported by the European Research Council (ERC: Starting Grant 309495-NeoNaNo) and by the German Research Foundation (LA 2937/1-2).

Funding European Research Council (ERC-StG-309495-NeoNaNo) and German Research Foundation (LA 2937/1-2).

Compliance with ethical standards

Conflict of interest S. Pochon is an employee of Bracco. F. Kiessling is co-owner of the invivoContrast GmbH and consultant of Bracco.

Ethic approval The retrospective use of formalin-fixed and paraffin-embedded human tissue was approved by the local ethics committee of the RWTH Aachen University.

References

1. Siegel R, Naishadham D, Jemal A (2012) Cancer statistics, 2012. CA Cancer J Clin 62:10–29. doi:10.3322/caac.20138
2. Ferlay J, Steliarova-Foucher E, Lortet-Tieulent J, Rosso S, Coebergh JW, Comber H, Forman D, Bray F (2013) Cancer incidence and mortality patterns in Europe: estimates for 40 countries in 2012. Eur J Cancer 49:1374–1403. doi:10.1016/j.ejca.2012.12.027
3. Berry DA, Cronin KA, Plevritis SK, Fryback DG, Clarke L, Zelen M, Mandelblatt JS, Yakovlev AY, Habbema JD, Feuer EJ, Cancer Intervention and Surveillance Modeling Network (CISNET) Collaborators (2005) Effect of screening and adjuvant therapy on mortality from breast cancer. N Engl J Med 353:1784–1792. doi:10.1056/NEJMoa050518
4. National Institute of Clinical Excellence (NICE) (2009) NICE clinical guideline 80. Early and locally advanced breast cancer: diagnosis and treatment. http://www.nice.org.uk/guidance/cg80. Accessed 18 Aug 2015
5. Deshpande N, Pysz MA, Willmann JK (2010) Molecular ultrasound assessment of tumor angiogenesis. Angiogenesis 13:175–188. doi:10.1007/s10456-010-9175-z

6. Abou-Elkacem L, Bachawal SV, Willmann JK (2015) Ultrasound molecular imaging: moving toward clinical translation. Eur J Radiol 84:1685–1693. doi:10.1016/j.ejrad.2015.03.016
7. Kranz A, Mattfeldt T, Waltenberger J (1999) Molecular mediators of tumor angiogenesis: enhanced expression and activation of vascular endothelial growth factor receptor KDR in primary breast cancer. Int J Cancer 84:293–298. doi:10.1002/(SICI)1097-0215(19990621)84:3<293:AID-IJC16>3.0.CO;2-T
8. Hood JD, Cheresh DA (2002) Role of integrins in cell invasion and migration. Nat Rev Cancer 2:91–100. doi:10.1038/nrc727
9. Somanath PR, Malinin NL, Byzova TV (2009) Cooperation between integrin $\alpha_v\beta_3$ and VEGFR2 in angiogenesis. Angiogenesis 12:177–185. doi:10.1007/s10456-009-9141-9
10. Pochon S, Tardy I, Bussat P, Bettinger T, Brochot J, von Wronski M, Passantino L, Schneider M (2010) BR55: a lipopeptide-based VEGFR2-targeted ultrasound contrast agent for molecular imaging of angiogenesis. Invest Radiol 45:89–95. doi:10.1097/RLI.0b013e3181c5927c
11. Bzyl J, Lederle W, Rix A, Grouls C, Tardy I, Pochon S, Siepmann M, Penzkofer T, Schneider M, Kiessling F, Palmowski M (2011) Molecular and functional ultrasound imaging in differently aggressive breast cancer xenografts using two novel ultrasound contrast agents (BR55 and BR38). Eur Radiol 21:1988–1995. doi:10.1007/s00330-011-2138-y
12. Bachawal SV, Jensen KC, Lutz AM, Gambhir SS, Tranquart F, Tian L, Willmann JK (2013) Earlier detection of breast cancer with ultrasound molecular imaging in a transgenic mouse model. Cancer Res 73:1689–1698. doi:10.1158/0008-5472.CAN-12-3391
13. Kiessling F, Gaetjens J, Palmowski M (2011) Application of molecular ultrasound for imaging integrin expression. Theranostics 1:127–134. doi:10.7150/thno/v01p0127
14. Yang M, Gao H, Yan Y, Sun X, Chen K, Quan Q, Lang L, Kiesewetter D, Niu G, Chen X (2011) PET imaging of early response to the tyrosine kinase inhibitor ZD4190. Eur J Nucl Med Mol Imaging 38:1237–1247. doi:10.1007/s00259-011-1742-z
15. Jin ZH, Furukawa T, Claron M, Boturyn D, Coll JL, Fukumura T, Fujibayashi Y, Dumy P, Saga T (2012) Positron emission tomography imaging of tumor angiogenesis and monitoring of antiangiogenic efficacy using the novel tetrameric peptide probe 64Cu-cyclam-RAFT-c(-RGDfK-)4. Angiogenesis 15:569–580. doi:10.1007/s10456-012-9281-1
16. Ehling J, Lammers T, Kiessling F (2013) Non-invasive imaging for studying anti-angiogenic therapy effects. Thromb Haemost 109:375–390. doi:10.1160/TH12-10-0721
17. Haubner R, Weber WA, Beer AJ, Vabuliene E, Reim D, Sarbia M, Becker KF, Goebel M, Hein R, Wester HJ, Kessler H, Schwaiger M (2005) Noninvasive visualization of the activated $\alpha_v\beta_3$ integrin in cancer patients by positron emission tomography and [18F]Galacto-RGD. PLoS Med 2:e70. doi:10.1371/journal.pmed.0020070
18. Yoon HJ, Kang KW, Chun IK, Cho N, Im SA, Jeong S, Lee S, Jung KC, Lee YS, Jeong JM, Lee DS, Chung JK, Moon WK (2014) Correlation of breast cancer subtypes, based on estrogen receptor, progesterone receptor, and HER2, with functional imaging parameters from ^{68}Ga-RGD PET/CT and ^{18}F-FDG PET/CT. Eur J Nucl Med Mol Imaging 41:1534–1543. doi:10.1007/s00259-014-2744-4
19. Iagaru A, Mosci C, Shen B, Chin FT, Mittra E, Telli ML, Gambhir SS (2014) (18)F-FPPRGD2 PET/CT: pilot phase evaluation of breast cancer patients. Radiology 273:549–559. doi:10.1148/radiol.14140028
20. Ehling J, Theek B, Gremse F, Baetke S, Möckel D, Maynard J, Ricketts SA, Grüll H, Neeman M, Knuechel R, Lederle W, Kiessling F, Lammers T (2014) Micro-CT imaging of tumor angiogenesis: quantitative measures describing micromorphology and vascularization. Am J Pathol 184:431–441. doi:10.1016/j.ajpath.2013.10.014
21. Rydén L, Linderholm B, Nielsen NH, Emdin S, Jönsson PE, Landberg G (2003) Tumor specific VEGF-A and VEGFR2/KDR protein are co-expressed in breast cancer. Breast Cancer Res Treat 82:147–154
22. Ghosh S, Sullivan CA, Zerkowski MP, Molinaro AM, Rimm DL, Camp RL, Chung GG (2008) High levels of vascular endothelial growth factor and its receptors (VEGFR-1, VEGFR-2, neuropilin-1) are associated with worse outcome in breast cancer. Hum Pathol 39:1835–1843. doi:10.1016/j.humpath.2008.06.004
23. Wang H, Cai W, Chen K, Li ZB, Kashefi A, He L, Chen X (2007) A new PET tracer specific for vascular endothelial growth factor receptor 2. Eur J Nucl Med Mol Imaging 34:2001–2010. doi:10.1007/s00259-007-0524-0
24. Anderson CR, Hu X, Zhang H, Tlaxca J, Declèves AE, Houghtaling R, Sharma K, Lawrence M, Ferrara KW, Rychak JJ (2011) Ultrasound molecular imaging of tumor angiogenesis with an integrin targeted microbubble contrast agent. Invest Radiol 46:215–224. doi:10.1097/RLI.0b013e3182034fed
25. Bzyl J, Palmowski M, Rix A, Arns S, Hyvelin JM, Pochon S, Ehling J, Schrading S, Kiessling F, Lederle W (2013) The high angiogenic activity in very early breast cancer enables reliable imaging with VEGFR2-targeted microbubbles (BR55). Eur Radiol 23:468–475. doi:10.1007/s00330-012-2594-z
26. Wells WA, Daghlian CP, Tosteson TD, Grove MR, Poplack SP, Knowlton-Soho S, Paulsen KD (2004) Analysis of the microvasculature and tissue type ratios in normal vs. benign and malignant breast tissue. Anal Quant Cytol Histol 26:166–174
27. Bluff JE, Menakuru SR, Cross SS, Higham SE, Balasubramanian SP, Brown NJ, Reed MW, Staton CA (2009) Angiogenesis is associated with the onset of hyperplasia in human ductal breast disease. Br J Cancer 101:666–672. doi:10.1038/sj.bjc.6605196
28. Vermeulen PB, Gasparini G, Fox SB, Colpaert C, Marson LP, Gion M, Beliën JA, de Waal RM, Van Marck E, Magnani E, Weidner N, Harris AL, Dirix LY (2002) Second international consensus on the methodology and criteria of evaluation of angiogenesis quantification in solid human tumours. Eur J Cancer 38:1564–1579
29. Riedl CC, Luft N, Bernhart C, Weber M, Bernathova M, Tea MK, Rudas M, Singer CF, Helbich TH (2015) Triple-modality screening trial for familial breast cancer underlines the importance of magnetic resonance imaging and questions the role of mammography and ultrasound regardless of patient mutation status, age, and breast density. J Clin Oncol 33:1128–1135. doi:10.1200/JCO.2014.56.8626
30. Mann RM, Balleyguier C, Baltzer PA, Bick U, Colin C, Cornford E, Evans A, Fallenberg E, Forrai G, Fuchsjäger MH, Gilbert FJ, Helbich TH, Heywang-Köbrunner SH, Camps-Herrero J, Kuhl CK, Martincich L, Pediconi F, Panizza P, Pina LJ, Pijnappel RM, Pinker-Domenig K, Skaane P, Sardanelli F, European Society of Breast Imaging (EUSOBI), with language review by Europa Donna-The European Breast Cancer Coalition (2015) Breast MRI: eUSOBI recommendations for women's information. Eur Radiol 25:3669–3678. doi:10.1007/s00330-015-3807-z
31. Joe BN, Sickles EA (2014) The evolution of breast imaging: past to present. Radiology 273:S23–S44. doi:10.1148/radiol.14141233
32. Berg WA, Blume JD, Cormack JB, Mendelson EB (2006) Operator dependence of physician-performed whole-breast US: lesion detection and characterization. Radiology 241:355–365. doi:10.1148/radiol.2412051710
33. Kaplan SS (2014) Automated whole breast ultrasound. Radiol Clin North Am 52:539–546. doi:10.1016/j.rcl.2014.01.002
34. Gasparini G, Brooks PC, Biganzoli E, Vermeulen PB, Bonoldi E, Dirix LY, Ranieri G, Miceli R, Cheresh DA (1998) Vascular

integrin alpha (v) beta3: a new prognostic indicator in breast cancer. Clin Cancer Res 4:2625–2634
35. Burke PA, DeNardo SJ, Miers LA, Lamborn KR, Matzku S, DeNardo GL (2002) Cilengitide targeting of $\alpha_v\beta_3$ integrin receptor synergizes with radioimmunotherapy to increase efficacy and apoptosis in breast cancer xenografts. Cancer Res 62:4263–4272
36. Desgrosellier JS, Barnes LA, Shields DJ, Huang M, Lau SK, Prévost N, Tarin D, Shattil SJ, Cheresh DA (2009) An integrin $\alpha_v\beta_3$-c-Src oncogenic unit promotes anchorage-independence and tumor progression. Nat Med 15:1163–1169. doi:10.1038/nm.2009
37. Seguin L, Kato S, Franovic A, Camargo MF, Lesperance J, Elliott KC, Yebra M, Mielgo A, Lowy AM, Husain H, Cascone T, Diao L, Wang J, Wistuba II, Heymach JV, Lippman SM, Desgrosellier JS, Anand S, Weis SM, Cheresh DA (2014) An integrin β_3-KRAS-RalB complex drives tumour stemness and resistance to EGFR inhibition. Nat Cell Biol 16:457–468. doi:10.1038/ncb2953
38. Desgrosellier JS, Lesperance J, Seguin L, Gozo M, Kato S, Franovic A, Yebra M, Shattil SJ, Cheresh DA (2014) Integrin $\alpha_v\beta_3$ drives slug activation and stemness in the pregnant and neoplastic mammary gland. Dev Cell 30:295–308. doi:10.1016/j.devcel.2014.06.005